Axonometric Inflation in Line Drawings Reconstruction

P.Company[1], J. Conesa[2] and N. Aleixos[1]

[1]Technology Department, Jaume I University, Castellon, Spain
[2]Polytechnic University of Cartagena, Spain

Abstract

A method suitable to automatically detect and reconstruct the *normalon* and *quasi-normalon* typologies is presented. Normalons are those particular polyhedrons where all edges in a corner meet at 90°, and all intersecting faces define a 90° dihedron. Quasi-normalons are those objects whose wireframe structure can be reduced to normalon by deleting some edges, without loosing any vertex. Many skeletons used to model mechanical parts and rough sketches of a large class of buildings belong to one those categories.

The method is based on the relationship between the angles defined by the orthogonal projections of three concurrent orthogonal segments and the angles that every one of those segments determine with its own projection. Hence, final models are obtained whenever the departure 2D line drawings are exact axonometric representations of normalons or quasi-normalons, and good tentative models are obtained in many other cases.

Key words: 3-D Reconstruction, Line Drawings Reconstruction, Visual Perception, Axonometric Drawings and Geometric Modelling.

1. Introduction

As was said many times before (Ullman, 1990; Cugini, 1991; Jenkins, 1993; Dori, 1993; Company, 1995), CAD systems have non-sequential (graphic) outputs, but accept only sequential (verbal) inputs. In the contrary, design process, and in particular conceptual design, needs non-sequential thought. Consequently, automatic solid-model generation from standardized Engineering Drawings is seen as an efficient way to establish a fluid communication between designers and CAD systems; at least in the present transition period from design-by-drawing to virtual prototyping paradigms. To go into this direction, automatic line-drawings reconstruction is one essential problem to solve.

Automatic line drawings reconstruction is now a well-established area in the Computer Vision field. For more than 30 years, since the pioneer work by Roberts (1963), some very different approaches have been presented. The works by Sugihara (1986), Nagendra and Gujar (1988) and Wang and Grinstein (1993), are good references to introduce the earlier advances.

In line drawings reconstruction, the input is a 2D line drawing, while the output is a geometrical three-dimensional model. We will use the term *drawing* to refer to the departure 2D line drawing, and *model* will be the wireframe, faces or solid models obtained when reconstruction takes place. Just wireframe and face models obtained from single axonometric view approaches are directly related to this paper.

Only "graph-like" drawings are considered during axonometric inflation. In other words, drawings must be made of line-segments (interpreted as projections of edges) and junctions (projections of vertices). The term *junction* will refer to a point were one line-segment ends, or two or more line-segments meet in the drawing. *Line-segments*, or simply *lines*, are the elements connecting two junctions in the drawing, while *edges* are the elements connecting two vertices in the model. The general point of view assumption applies: each junction in the graph represents one and only one vertex in the model, and each line in the

drawing represents one and only one edge in the model. Finally, no difference is made in the drawing between visible and non-visible edges, and all edges must be drawn.

1.1 Normalon and quasi-normalon typologies

While in the past the objective was a general approach aimed to reconstruct a general class of models, nowadays the need to classify models in specific and useful typologies is recognized. Recently, some methods designed to cope with specific typologies, like minimal origami (Parodi, 1996), have been developed, because it is assumed the reconstruction is more effective when a particular approach is fitted to the model typology. In our approach, a main restriction also applies to the nature of the model, because only normalon polyhedrons are considered.

The name is a generalization to the polyhedrons 3D world of normalon polygons, defined by Dori (1992) as those having the property that the angle between any two adjacent sides is 90º. *Normalons* are those particular wireframes or face models where exactly three edges meet in every corner and they do at 90°. Consequently, every pair of intersecting faces defines a 90° dihedron. The typology is suitable to be easily extended to *quasi-normalons*; defined as those objects whose wireframe structure can be reduced to normalon by deleting some edges, whilst ensuring no one vertex is loosed during the process and any disconnected subgraphs appear.

There are many examples in the line drawings reconstruction literature where normalons and quasi-normalons appear (Marill, 1991; Lipson and Shpitalni, 1996; Leclerc and Fischel, 1992) (see figure 1).

(a)

(b)
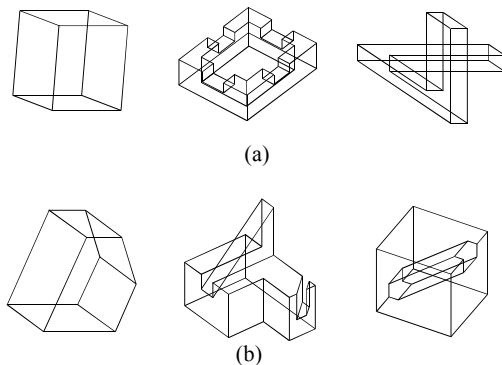
Figure 1: *Some (a) normalons, and (b) quasi-normalons appeared in line drawings reconstruction literature.*

The typology is not so restrictive as it seems at first glance, because sketches of many skeletons (or "control structures") used to model complex mechanical parts in 3D CAD modelling systems (see figure 2), and many sketches of architectural buildings (Turner et al, 2000) (see figure 3), belong to this category.
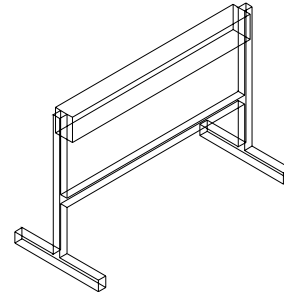
Figure 2: *Normalon skeleton.*
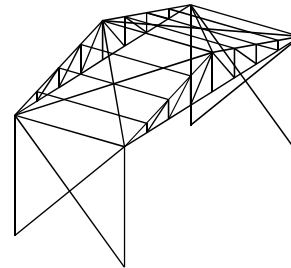
Figure 3: *Quasi-normalon building structure.*

1.2 Related work

The clearest antecedent to the Axonometric Inflation was the approach by Lamb and Bandopadhay (1990). Lipson and Shpitalni (1996) also presented a strategy for accelerating and improving convergence in "orthogonal" (normalon) models. In their approach, lines in the sketch are associated with one of the three orthogonal directions, and vertex positions are computed starting at an arbitrary origin point with an arbitrary depth of zero and advancing to adjacent points using lines parallel to the three orthogonal directions.

The entire process described by Lamb and Bandopadhay included a tiding phase, where input drawing was converted to a graph-like drawing. Then one group of main axes (x, y, z) was given as input. Next, labelling and face detection were automatically done, and candidate faces, or "regions", were obtained. Any face parallel to one coordinate plane was considered as "main" face, while the rest were "oblique". In the core phase, the coordinates of any point in the object could be obtained by calculating

the distance, along the x, y and z axes, between this point and the origin. Likewise, if the coordinates of one point were known, the coordinates of adjacent points could be derived relative to the known point. The system exploited this concept to determine all the coordinates of an object relative to the junction selected as the origin (figure 4).

Holes and protrusions (i.e. disconnected subgraphs) could also be solved; provided the labelling and face detection process were able to identify whether faces happened, and which was the contact face; because the object part indicated by the subgraph contacts the rest of the object at a surface, rather than an edge.
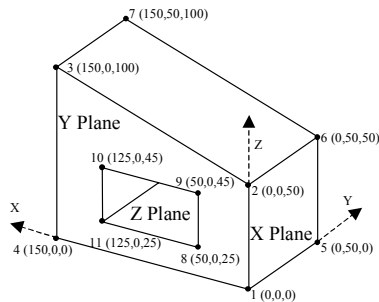
Figure 4: Example of Lamb and Bandopadhay, where main and oblique planes, main axis and coordinate propagation can be seen.

The bases of the approach by Lamb and Bandopadhay are parallelism and proportionality relations in axonometric views. They are two well-known invariants in parallel projections. In particular, all axonometric views (both, orthogonal and oblique) inherit those properties, which are intensively used in traditional line drawing.

Nevertheless, the approach is not geometrically consistent, because they are the *inverse* of those properties that are applied: a) whenever two lines are parallel in the drawing they *must* correspond to two parallel edges in the model, and b) two proportional segments in the drawing *must* always correspond to two proportional edges in the model. Hence, by assuming reconstruction to be the inverse of projection, parallelism and proportionality relations are heuristically extended from univocal to biunivocal properties.

In other words, the approach is heuristic because those inverse rules are perceptual, rather than geometrical properties. Therefore, the approach will work if, and only if, the typology of the object ensures such rules to be accomplished. Consequently, in the approach by Lamb and Bandopadhay, although they do not explicitly declare the point, the model

must be a normalon or a quasi-normalon. Even then, quasi-normalons would be here considered as those face-models that can be reduced to normalon like by temporarily eliminating as much oblique faces as needed.

However, maybe the most important limitation in the approach is the need to detect faces before reconstruction. This is not a trivial task, because, only two-dimensional information contained in the original drawing can be used (Shpitalni and Lipson, 1996). This is why using only what Varley and Martin (2000) named "frontal geometry" simplifies notably the problem. According to Lamb and Bandopadhay hidden lines are a problem because: "unless they can provide information about unseen structure of an object, they also add a number of ambiguities to a drawing". Certainly, the problem was solved because frontal geometry simplified face detection, and allowed geometrical reconstruction. In addition, the full geometrical model was later obtained, because after reconstruction another algorithm was used to infer the hidden structure of the object. Nevertheless, creation of hidden faces was only possible for simple shapes, and no option was left for the user to sketch hidden lines to improve the description of complex objects in order to avoid misinterpretations.

The second antecedent to the Axonometric Inflation comes from the very well known dependence linking the axonometric coefficients (e_x, e_y, e_z) and the angles between every pair of the reference axis projections ($X\hat{O}Y$, $X\hat{O}Z$, $Y\hat{O}Z$).

It is described in nearly every standard Descriptive or Constructive Geometry texts (Hohenberg, 1956) (most of which go back to Polkhe's Theorem) in which way a dependence can be established between the angles defined by the orthogonal projections of three concurrent orthogonal segments and the angles that every one of those segments determine with its own projection. However, in classical references, the problem was always graphically solved. We, instead, can go back to Perkins (1971), or Attneave and Frost (1969), to find its analytical formulation, applied to solve visual perception problems. Perkins studied the bearing of projective geometry on the perceptual processes by which pictures are "read" for spatial information. To be noticed that Perkins emphasized the logical ambiguity of line drawings (their lack of distinct three-dimensional information), together with the active role of the visual system in making assumptions to resolve this ambiguity. Attneave and Frost used that formulation to explore the differences

between perceived and geometrical depth and orientation.

To sum up, we take profit from previous formulations to determine the angle (for instance ϕ_Z) between every edge (OZ) and its own line-segment (O'Z') when three orthogonal edges are connected to the same central vertex (see O in figure 5). It is a function of the angles (X'Ô'Z' and Y'Ô'Z') between the orthogonal projection of OZ (O'Z') and the orthogonal projections of the other two orthogonal edges (O'X' and O'Y'):

$$\sin \phi_Z = \sqrt{\cotg (X'\hat{O}'Z') \cdot \cotg (Y'\hat{O}'Z')} \qquad (1)$$

(a)   (b)
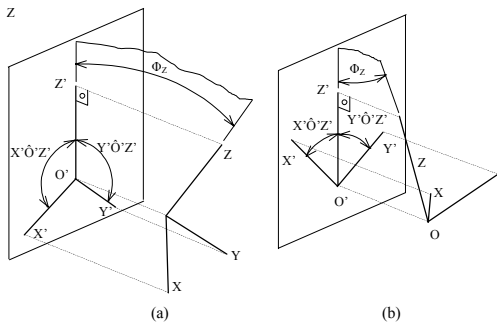
Figure 5: *Dependence between the angles in the orthogonal projection of an (a) "Y" type and (b) "W" type of an orthogonal thriedron.*

It can be noticed that the axonometric coefficient would be $e_Z = O'Z'/OZ = \cos \phi_Z$.

Finally, the problem of main directions will be considered. The reconstruction method proposed by Lamb and Bandopadhay requires users to interactively determine the projections of the reference axis. However, Lipson and Shpitalni (1996), proposed a heuristic strategy for obtaining prevailing angles and main directions. The *angular distribution graph* (ADG) allows automatic detection of main axis. In their own words: "It is possible to identify the main axis directions of the intended object from this graph."
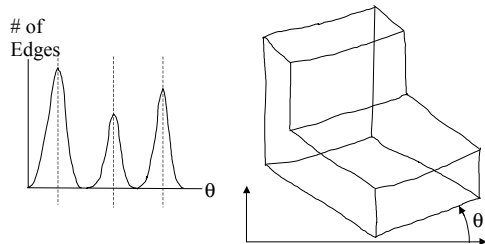
Figure 6: *Angular Distribution Graph to identify the main axis directions.*

The ADG is constructed by sampling the angle of every line-segment in the drawing and plotting it on an angular distribution histogram. The ADG is filtered to account for the inaccuracy of the sketch (a Gaussian distribution curve, with s= 7°, is superimposed onto the ADG and the graph is normalized with its maximum to 1.0). The resulting ADG qualitatively shows the prevailing angles in the drawing. As shown in figure 6, three dominant angles appear in strictly orthogonal objects (normalons).

1.3 Inflation process

Inflation, or backprojection, is, roughly speaking, the inverse of projection. The process is shown in figure 7 and is based on the following key ideas:

a) A univocal correspondence is established between vertices in the model and junctions in the drawing. Every junction does correspond to one, and only one, vertex.

b) A univocal correspondence is established between edges in the model and line segments in the drawing. Edges do connect those vertices whose corresponding junctions are connected by its corresponding line-segment.

c) A Cartesian coordinate system is defined, and the XY coordinate plane is made coincident with the drawing plane; then, a transformation is defined to ensure (X, Y) coordinates of every junction in the drawing to be equal to (X, Y) coordinates of the corresponding vertex in the model.
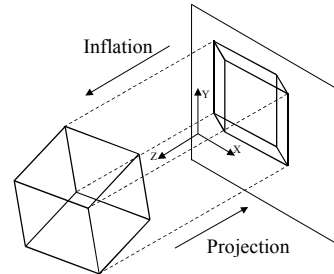
Figure 7: *Inflation of a wireframe from a line drawing.*

Thus, each model obtained by inflation is characterized by a set of coordinates $\mathbf{z} = (z_1, z_2,...,z_n)$. Where the number of vertices n determines the *order* of the problem. Obviously, it is an infinite number of "valid" sets of coordinates, and the key for inflation to give "good" models depends on the strategy used to choose the "right" set. Our own strategy to obtain the good model is presented next.

2. Axonometric Inflation of an orthogonal corner

Let us suppose an orthogonal projection of an orthogonal corner like A'B'C'D' in figure 8. To reconstruct the model (i.e. to determine x, y and z coordinates of vertices A, B, C and D) the Cartesian coordinate system associated to inflation is used to trivially obtain x and y coordinates of all four vertices ($x_A = x_{A'}$, $y_A = y_{A'}$, …).
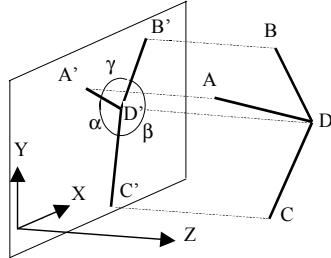
Figure 8: *Axonometric Inflation of an orthogonal corner.*

Next, z coordinates of lateral vertices (A, B, C) are related to z coordinate of central vertex (D) through the following relation:

$$|z_C - z_D| = L_{C'D'} \cdot \tan \phi_C \qquad (2)$$

As shown in figure 9, $L_{C'D'}$ is the length of C'D' line segment (CD edge projection), and z_C and z_D are the respective z coordinates of both vertices in the reconstructed edge. Obviously, ϕ_C can be obtained from (1), simply substituting X'Ô'Z' and Y'Ô'Z', by α and β.
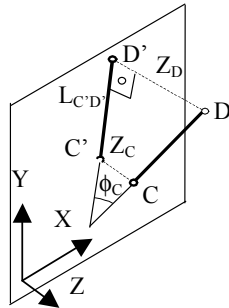
Figure 9: *z coordinates as a function of ϕ angle.*

The coordinate z_C obtained from (2) is relative to the z coordinate of vertex D. Nevertheless, for reconstruction purposes the z coordinate of vertex D can be arbitrarily fixed without loss of generality, because the trihedral shape will be the same, only its position will be different.

The solution is still not unique, because there are two possible values for z_C (figure 10):
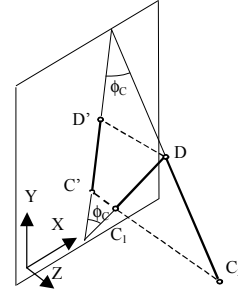
Figure 10: *Two alternative inflations.*

$$z_C = z_D \pm L_{C'D'} \cdot \tan(\mathrm{asin}(\mathrm{cotg}(\alpha) \cdot \mathrm{cotg}(\beta)))^{1/2}) \qquad (3)$$

A reversion of all three edges in the corner would lead to a second valid solution: the well-known Necker's reversion shown in figure 11.
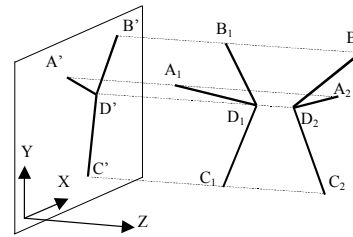
Figure 11: *Necker's reversion in the inflation.*

As both corners in figure 11 are valid, no one criterion is applied to choose one of them. Both are offered to the user. Nevertheless, some obviously invalid corners can appear if plus or minus signs are randomly chosen when (3) is used to determine all three lateral vertices. To avoid undesired solutions a subsequent check is made.

One of the two Necker solutions is selected when one of the two alternatives for the *first edge* is freely chosen (for instance D_1C_1 or D_2C_2). Notice that maintaining the consistence of the edge determined first will be of capital importance in the approach. Next, equation (3) is solved for one secondary edge with and arbitrary sign. For instance the + sign is assigned to obtain:

$$z_A = z_D + L_{A'D'} \cdot \tan(\arcsin(\sqrt{\mathrm{cotg}(\beta) \cdot \mathrm{cotg}(\gamma)})) \qquad (4)$$

Then, to ensure a consistent and valid solution, the angle between the secondary edge (AD) and the first edge (CD) is checked to be 90º. If the angle differs from 90º in less than a tolerance value, the coordinate z_A is fixed; otherwise, the alternative sign is adopted:

$$z_A = z_D - L_{A'D'} \cdot \tan(\arcsin(\sqrt{\mathrm{cotg}(\beta) \cdot \mathrm{cotg}(\gamma)})) \qquad (5)$$

The process is repeated for the other secondary edge (BD), and a final check for the angle between second

and third edges to be 90º is made to ensure consistence.

This process is entirely consistent with the human strategy of abandoning interpretations found inconsistent and trying some alternative. It is the hypothesis-making and hypothesis-testing process, described in many human and machine perception documents.

2.1 Limitations in the approach

Equations 1 to 5 are valid for both "Y" and "W" type of orthogonal projection of an orthogonal corner (figure 12).

(a)   (b)
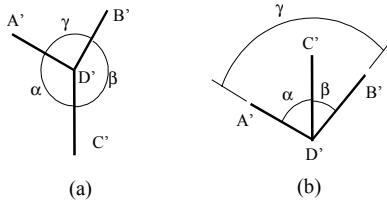
***Figure 12:** Corners of (a) "Y" and (b) "W" typologies, and their angles.*

The angles measured in the image are always in the range [0º, 180º]. Moreover, the projective consistence for trihedral orthogonal corners states that for a pictured corner to be the orthogonal projection of a solid rectangular three-dimensional corner, all three angles around the corner must be greater than 90º in the "Y" type. And two angles around the corner, each less than 90º, must sum to greater than 90º in the "W" type (see, for example, Perkins, 1976).

For the "Y" type corner, it is meaningless which one of the three lines act as first edge: in all cases, the two angles used in (3) will be in the range [90°, 180°]. However, in the "W" type, both angles are in the range [0°, 90°] only if the first edge is the central edge (C'D' in figure 12). If any of the two other edges is used as central ("W" type with lateral first edge), one of the two cotangents will be positive while the other will be negative, and this will cause a numerical error in (3).

Furthermore, analysing the real domain of expression (3), it can be observed that the function is undefined for values of α and β that satisfy either of the following two conditions:

$$|\cot \alpha \cdot \cot \beta| > 1 \qquad (6)$$

$$\cot \alpha \cdot \cot \beta < 0 \qquad (7)$$

The expression (6) can be reformulated as:

$$|1 + \cot(\alpha+\beta) \cdot (\cot \alpha + \cot \beta)| > 1 \qquad (8)$$

or

$$\cot(\alpha+\beta) \cdot (\cot \alpha + \cot \beta) > 0 \qquad (9)$$

In other words, if both the cotangent of the sum and the sum of cotangents have the same sign, the expression (3) will not have value in the real field and therefore Axonometric Inflation cannot be applied. In the "Y" type, the sum of cotangents is negative (α and β are always greater than 90°), consequently (9) will only be positive if the third angle ($\gamma=\alpha+\beta$ in the figure 13) is less than 90°. It is not an important limitation because, as was said before, this may not correspond to any orthogonal projection of an orthogonal corner. In the same way, the "W" type will work if the first edge is the central edge and the junction accomplishes the orthogonallity rule (α and β are less than 90º, and γ greater than 90º). To know what happens when a lateral edge is the first edge, let us analyse the condition given in (7).

The condition given in (7) will be verified when one of the two cotangents is positive and the other is negative. This occurs in the "W" type with lateral first edge described above. They may also appear when central edge is the first edge, and one angle (α or β) is greater than 90° and the other is less than 90°. Again, this second case may not correspond to any orthogonal projection of an orthogonal corner. Nevertheless, in our attempt to solve the "W" type with lateral first edge, we solved both cases, because we avoided the numerical restriction by simply substituting the cotangent of the angle greater than 90° by its absolute value. This is equivalent to substitute the angle by its supplementary; i.e. in figure 13, the line-segment A'D' is substituted by $A'_{eq}D'$.

(a)   (b)
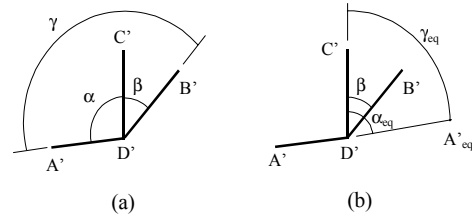
***Figure 13:** "W" type corner, with (a) one angle greater than 90º, and (b) the equivalent corner.*

As both segments are in the same line, the same ϕ angle is obtained. In other words, the angle between line segment AD and its projection A'D' is the same defined by the line segment $A_{eq}D$ and its projection (figure 14).
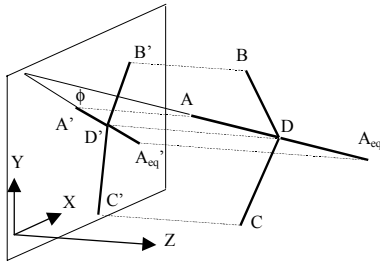
Figure 14: *One "Y" type and its equivalent "W" type corner.*

The particular case where the two angles come to 90° (a "T" type) does correspond to a degenerate point of view where a face (ADB) is orthogonal to the drawing or "projection" plane (i.e. the AC edge is parallel to the projection plane); hence $\phi_Z = 0$.
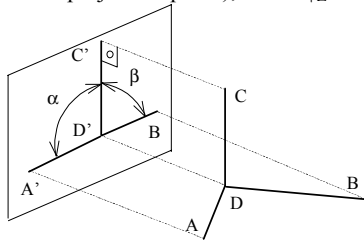
Figure 14: *"T" type of orthogonal projection of an orthogonal thriedron.*

Nevertheless, this particular case is dangerous, because z coordinates are trivially assigned, but a false collinearity (OX and OY) may be detected, and can result in incorrect assumptions. However, is a degenerated case, with no practical interest, because it corresponds to a non-general axonometry, where faces parallel to XOY plane degenerate in lines.

The degenerated case where any of the two angles is 180° is also restricted.

Finally, the particular cases when only one of the angles is 90° or 135° (like cavalier axonometry), can be solved using an artifice to obtain a tentative model. To avoid numerical run-outs, we simply modify conflictive angles adding a threshold to avoid numerical run-outs. In this way, numerical calculation give a finite value, and the resulting model is topologically quite good, although its dimensions are notably incorrect.

3. Propagation of axonometric inflation

The Axonometric Inflation of an orthogonal corner, described in previous section, can be easily extended to determine all vertices of complex normalon and quasi-normalon models by successively calculating as much corners as are necessary to finally determine all vertices in the model.

However, the successive corners cannot be accidentally chosen. Propagation is the way to ensure that relative coordinates of every corner are converted to the same absolute coordinates in the model. Hence, a *propagation tree* is needed. We use a particular version of Kruskal algorithm to obtain a spanning propagation tree formed by all edges connecting the successive central vertices. The lateral vertex connected through the longest edge is defined as the central vertex for the new corner; because it is assumed that longer edges are less prone to error than shortest do (i.e. the dimensional relative errors are minor, and long lines are more accurately drawn in hand drawing). The process is repeated until all vertices in the model have been determined. In case where converting any of the present lateral vertices in central ones would generate a circuit (i.e. if all lateral vertices have been previously visited) the branch is abandoned and the longest lateral edge not yet explored is used to begin a new branch.

For example, in the drawing of figure 15, vertex V_0 was chosen to begin the tree. Using vertex V_0 as central, V_1, V_2 and V_3 were calculated. Then V_3 acted as central (because it was in the longest edge departing from V_0), and V_5 and V_6 were obtained. Nor V_5, neither V_6 allowed calculation of any still not visited vertices. Hence, the branch was abandoned and a new one, starting at V_1, allowed V_4 to be obtained. As all vertices had been visited, the process ends.
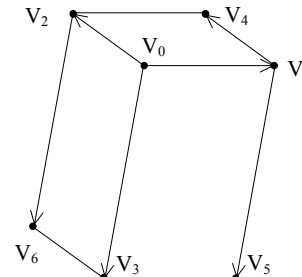
Figure 15: *Propagation tree of absolute z coordinates.*

Notice that in order to prevent undesired Necker reversions during propagation, the edge connecting previous central vertex with new central vertex must be always adopted as first edge for the new corner.

Finally, to detect possible ill working, due to a bad selection of propagation trees, a check is made after the final model has been obtained. If the final model

is a non-normalon, the tree-nodes corresponding to the central vertex from which the non tri-rectangular vertices were calculated, are marked as non-valid as central vertices, and a new reconstruction is attempted trough an alternative propagation tree. In case that neither a valid model can be obtained, the best tentative model will be delivered and the user should be informed about its flaws.

As faces information is not required in Axonometric Inflation, the approach can be easily extended to reconstruct quasi-normalon models, like the one in figure 16. The temporary elimination of all line-segments that are non-parallel to any of the three main directions determines a normalon, which is *equivalent* if any vertex disappears during the conversion and the graph is still connected.
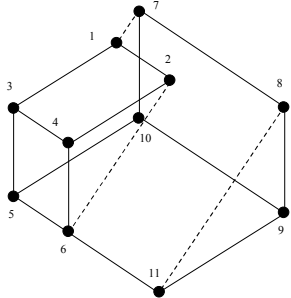
Figure 16: *Transformation from quasi-normalon, to equivalent normalon, by deleting dotted lines.*

3.1 Extension to models of other valences

It must be highlighted that the algorithm requires three orthogonal edges concurring in every central vertex. Nevertheless, the restriction applies *only* to central vertices. The *valence* (the number of edges concurring in a vertex) of lateral vertices is irrelevant. Consequently, the approach will work if a propagation tree can be obtained where all central vertices have a valence of three, and, thus, all vertices of other valences can be determined as laterals. In other words, Axonometric Inflation can be applied to the "extended" class of polyhedrons whose propagation tree is normalon.

For instance, in figure 17, 10 is selected as the departure vertex. Starting from it, the coordinates of the vertices 5, 7 and 9 can be determined. Then, 9 should be the next central vertex. It will allow 8 and 11 to be calculated. However, when continuing the process, nor 11, neither 8 can be central as long as its valence is two. The evaluation continues opening the branch connecting 10 to 5, which allows vertices 3 and 6 to be obtained. Then, we move to central vertex

6, to determine vertex 4. A new move to 4 allows the calculation of 2. Finally, the evaluation of vertex 1 is carried out through the vertex 3, concluding the definition of the model.
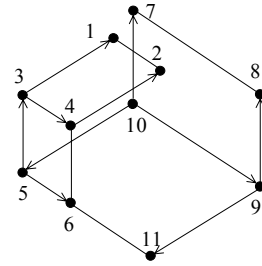
Figure 17: *Propagation tree, in which all central vertices have valence 3.*

It may happen that, in spite of getting an equivalent normalon, Axonometric Inflation cannot be applied if certain vertices are not accessible through some valid propagation tree. This is the case when some junctions are only connected to other junctions of valence less than three. For instance, in figure 18, vertex 3 is only connected to vertex 4, which cannot be central because its valence is two. The same happens to vertices 6 and 7.
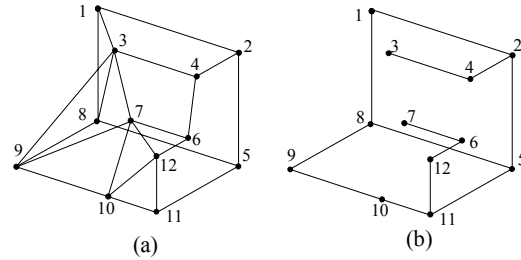
Figure 18: *First transformation: from (a) quasi-normalon, to (b) non-solvable normalon.*

When the valence of a central vertex is less than three, equation (3) cannot be used, because one or two of the angles (α, β) are undefined. Nevertheless, the assumption of the model to be a normalon has already been made. Hence, adding fictitious line-segments is coherent with the assumption and solves the problem. Those fictitious line-segments are defined of unit length and oriented in accordance with those main directions still not present in the vertex. In figure 19, fictitious edges $4-F_1$, $12-F_2$ and $6-F_3$ allow vertices 3, 6 and 7 to be determined.
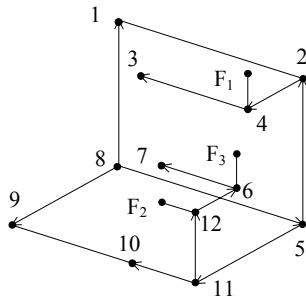
Figure 19: *Solvable equivalent normalon.*

When vertices of valence greater than three appear, the approach will still work if a valid propagation tree can be obtained; i.e. a tree where those vertices are not central. When this is not possible, we have confined ourselves to obtain one of the potential models, by randomly choosing three of the edges that converge in the vertex.

3.2 Extension to collinear edges

A problem occurs in those central vertices where collinear edges converge. In fact, two situations may happen. In the first (illustrated in figure 20), let us suppose AD (or BD) is the first edge. A simple proportionality calculation will allow the determination of vertex B (or A), but the z coordinate of vertex C cannot be obtained. Applying the standard procedure (equation 3), the value of the angle φ is determined from the angles defined by the line-segment D'-C' with the line-segment D'-A' and D'-B'. The possible coordinates for the vertex C are determined by the expressions (4) and (5), what results in the vertices C_1 and C_2. Notice that, as CD must be perpendicular to both AD and BD, and AD and BD are collinear, the plane C_1DC_2 is perpendicular to the line AB. Hence, the edges DC_1 and DC_2 are both orthogonal to the edges DA and DB. Therefore, the perpendicularity check, where the angle between the third edge (CD) and the first edge (AD) is checked to be 90º, cannot solve the undetermined. The only solution would be to add a fictitious edge. In a similar way, it can be concluded that, if CD is the first edge, nor AD neither BD can be determined unless one fictitious edge is added.
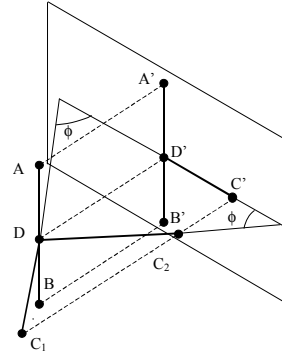
Figure 20: *Lack of determination in the Axonometric Inflation of collinear edges.*

Therefore, in the selection of the propagation tree, vertices with collinear edges are simply considered as having a reduced equivalent valence. For instance, in the figure 21 vertices 2 and 5 have an equivalent valence of 2 (i.e. 4 edges, minus 1 oblique, and minus 1 collinear).

Nevertheless, we can take advantage of the particular situation when the first edge is the collinear. Then, calculation of the third collinear vertex is possible. For instance, 1 can be determined if the edge 2-3 is known.
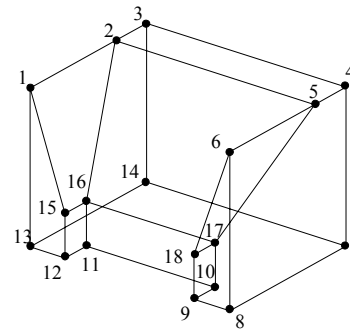
Figure 21: *Drawing with collinear edges.*

It can be seen that in the evaluation of this drawing, the lines 1-2 and 2-3, and the lines 4-5 and 5-6 are collinear. Hence, initially vertices 2 and 5 cannot be used as central. In other words, the vertex 5 will be evaluated starting from the vertices 4 or 6, and the vertex 2 will be evaluated in an independent way starting from the vertices 1 or 3.

3.3 Extension to false parallel edges

Accidental points of view can cause erroneous detections of non-normalons as normalons or quasi-normalons. Such a case happens if two non-parallel edges are accidentally projected as parallel lines in

the drawing. The figure 22 shows an example where the edge 5-6, would be considered parallel to the edges 1-4, 2-3 and 7-8, although it should be really interpreted like crossing edges.
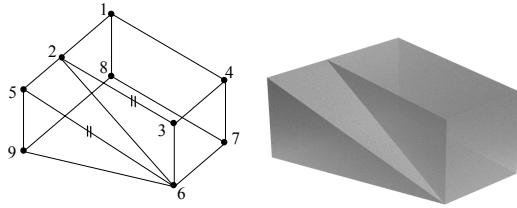
Figure 22: *(a) Model prone to (b) false edge parallelism due to a particular point of view.*

In this case, vertex 2 has an equivalent valence of 2 and is avoided in the propagation tree. Hence, the "correct" reconstruction is obtained.

Other false parallel edges (like V_1V_2 and V_1V_3 in figure 23) can cause ill working that is only detected in the final check made after the model has been obtained. In the drawing of figure 23a, two accidental parallel conditions happen. As a result, vertex V_1, is erroneously considered as having an equivalent valence of 3, and can be used as central vertex; resulting in a model like the one shown in figure 23b; where vertices V_1 and V_2 would be detected as a non orthogonal and the invalidation process described above will be fired.

(a)   (b)
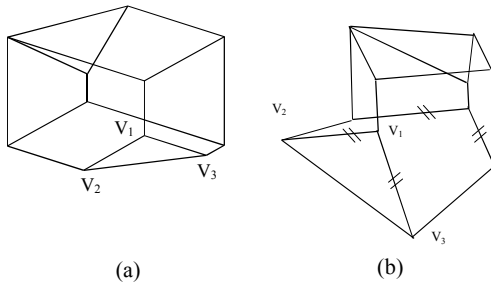
Figure 23: *Quasi-normalon represented in (a) a drawing with false parallel lines and (b) its incorrect reconstruction.*

4. Main directions

Automatic detection of main directions is of capital importance for Axonometric Inflation. First, it is important to decide whether a drawing represents a normalon, because the decision is made by checking if three and only three main directions are present in the drawing. Second, because main directions are used to determine axonometric axis.

4.1 Automatic detection of main directions

The methodology proposed by Lipson and Shpitalni (the *angular distribution graph*) was adopted to determine main directions. Nevertheless, at present a simplified version is used, because our input drawings are "perfect" (both because they are initially drawn with a drawing CAD tool, or because they are tidied in a pre-processing step). Hence, three main directions are determined by simply counting the number of line-segments that are parallel to each other. To prevent round offs, a threshold of 3º is used to decide whether a line segment is to be considered parallel to other. Then, the three more frequent are selected as main directions. In other words, they are considered main directions those that appear most times in the drawing. An additional check is made to ensure that junctions with those three directions exist. In the figure 24, a model proposed by Lipson and Shpitalni shows four directions and their frequencies.
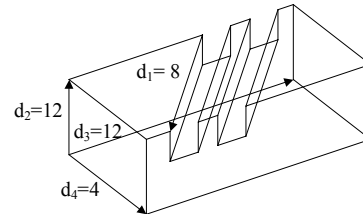
Figure 24: *Quasi-normalon with four directions.*

Sometimes, the process described above results in an erroneous choice of main directions. In the figure 24, the combination $(d_1 \ d_2 \ d_3)$ would be selected, since their frequencies are greater than the one given by the direction d_4, and junctions with those three directions exist. Consequently, the reconstructed model would be the one shown in figure 25.
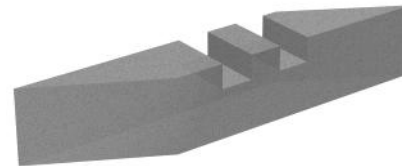
Figure 25: *Perceptually erroneous reconstruction.*

Perkins (1976) demonstrated that perceptual rules are restrained by projective geometry. This means that projectively impossible regularities are not used in human perception. The rule of projective consistence for trihedral orthogonal corners were mentioned above: for a pictured corner to be the projection of a solid rectangular corner in space, either all three angles around the corner must be greater than 90º or two, each less than 90º, must sum to greater than 90º. The rule applies equally to parallel and perspective

projection, so long as the line of sight is approximately perpendicular to the picture surface. Hence, checking the projective consistence is the main criteria to detect false main directions (figure 26).
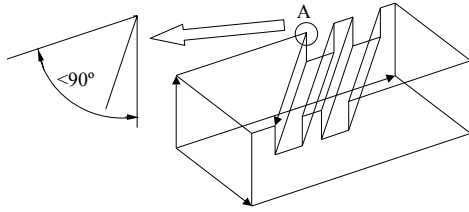
Figure 26: Projectively impossible orthogonal corner.

Applying this rule, the combination (d_1 d_2 d_3) would be rejected due to the vertex A to be a projectively impossible orthogonal corner. The combinations (d_1 d_2 d_4) and (d_1 d_3 d_4) would be rejected because they are not present in any vertex (i.e. they are topologically incorrect). Only the combination (d_2 d_3 d_4) would be accepted.

Finally, to improve the selection process, two perceptual rules are applied: for the same frequency, longest lines are preferred, and combinations including directions parallel to contour edges are explored first.

As was said before, the edges in normalons are oriented according to three and only three directions. Hence, this seems a good criterion to discriminate whether the model is a normalon. Unfortunately, the opposite is not always true, i.e. sometimes three main directions do not correspond to three-dimensional edges of a normalon model. For instance, the model shown in figure 27, proposed by Lamb and Bandopadhay, would be classified as quasi-normalon, instead of prismatic, because one of the three vertices A_1, A_2 or A_3 would be considered as an orthogonal corner.
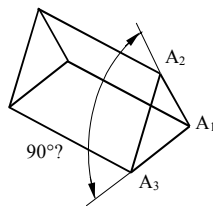
Figure 27: False orthogonallity.

Unfortunately, checking for projective consistence can help to reject some of the false orthogonal corners in figure 27, but not all three would be

rejected. Face detection would be required to discriminate such cases.

4.2 Axonometric axis

After reconstructing by Axonometric Inflation, the resulting model is referred to the *Inflation coordinate system* (see $O_I X_I Y_I Z_I$ in figure 28). However, an axonometric reference system would be better.

In the approach by Lamb and Bandopadhay, the *Front Axonometric System* ($O_F X_F Y_F Z_F$) is implicitly adopted, because the largest region is considered first, and the lower left junction is assigned as the reference vertex. Hence, the reference vertex is implicitly assigned as the one with the lowest position in the best face, which is the one contained in a main plane and with the biggest line-segment. This choice has a rough geometrical meaning. It assumes that the origin is in front of the model, the model is being observed from an upper point of view, and the origin is in the "ground" or base plane (the plane XOY, because vertex Z is considered vertical).
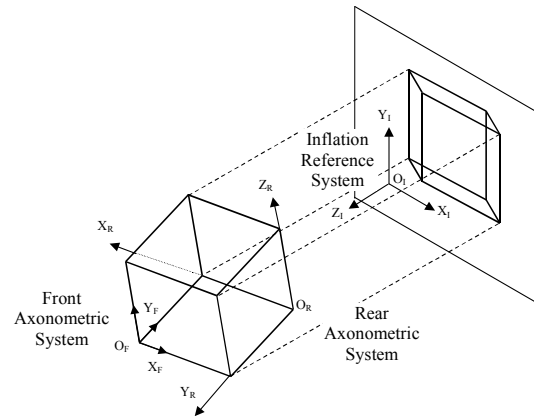
Figure 28: Reference Systems in Axonometric Inflation.

In our approach, Inflation Reference System was used to reconstruct, and a post-processing applied to finally reference the model to the Rear Axonometric System.

In order to determine the Rear Axonometric System, the three main directions must be previously determined. Then, as long as the same geometrical assumptions described above are made, the origin (O_R) is made coincident with one vertex in the graph of inverted Y typology, as close as possible to the geometric centre of the graph, and connected to the largest line segments. If the previous three conditions

are incompatible, the order in which they are listed above indicates their priority.

5. Results

Axonometric Inflation has been implemented and tested on a program called REFER, that is being developed by the authors. C++ is used to implement the calculations and data management; Graphical User Interaction is achieved by calling win32 operations through Visual C++, and Open GL was chosen as the best alternative to visualise 3D models.

The input data is a drawing made of line-segments and junctions, supposed to be some kind of axonometric orthogonal projection of a normalon or quasi-normalon model. The drawing is a graph-like stored in DXF or IGES format. The output is also a DXF or IGES format containing a wireframe or surface model, because face detection can be done separately.

The algorithm has proved valid for all normalon of valence 3, and almost all type of quasi-normalons, in more than two hundred models like those shown in figure 29.
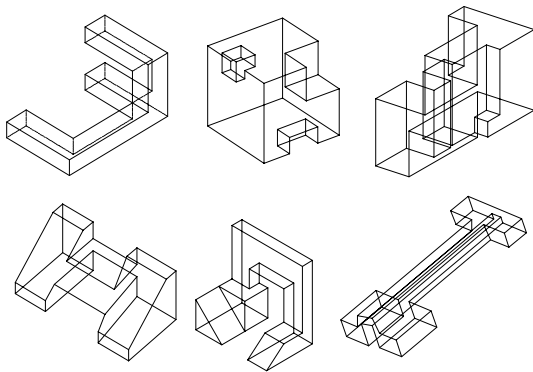
Figure 29: Some drawings reconstructed with REFER.

Strictly speaking, Axonometric Inflation is only valid when the image corresponds to an orthogonal axonometric projection. Nevertheless, for certain oblique axonometric views where the projection does not deviate excessively from orthogonal, the proposed method does succeed in reconstructing approximate models.

As was said above, in Cavalier's axonometric views (figure 30), Axonometric Inflation is unable to obtain any model. Nevertheless, an artifice consisting in arbitrarily adding a threshold to conflictive angles is employed. The values proposed are 91º instead of 90º

and 134º instead of 135º. A threshold minor than 1º enlarges oblique faces; i.e. proportion L/H in figure 30 is clearly greater than perceived proportions in the Cavalier drawing. In the other hand, a greater threshold rapidly increases local distortions (like the one observed in vertex A in figure 30).
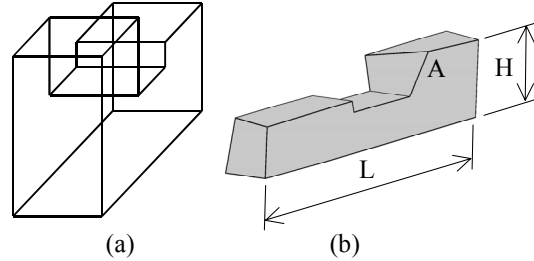
Figure 30: Normalon model in (a) a Calavier drawing, and (b) a view of its "tricky" reconstruction by Axonometric Inflation.

To sum up, the Axonometric Inflation will give exact results only when applied to normalon models, projected according to orthogonal and parallel projections. Under such conditions, perfect models are obtained, and none refinement procedures are required.

Nevertheless, when applied to non-normalon polyhedral, or when applied to non orthogonal projections where the line of sight is almost orthogonal, the resulting 3D model is still useful to obtain *tentative models*, which can be used as departure models to carry out an optimisation process. As was said elsewhere (Conesa et al, 1999), tentative models are useful in optimisation approaches, because they allow beginning the optimisation process very close to the global optimum, escaping from local optima (figure 31).
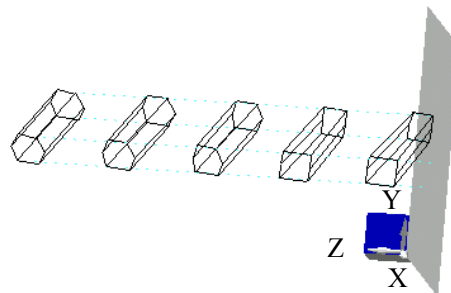
Figure 31: Reconstruction by optimisation ,beginning from a tentative Axonometric Inflation model.

6. Conclusions

Due to the great variety of models to be reconstructed, a general approach for automatic solid-model generation from engineering drawings has proved to be inefficient. Consequently, the "divide and conquer" strategy is adopted.

The heuristic inflation rules seem to be a good approach to directly solve some simplest models. They may also serve to get departure models, which improve efficiency in other approaches, like the optimisation process based on regularities; where departing from the drawing constitutes a real problem, since it is a local minimum.

One of such heuristic approaches is Axonometric Inflation, which allows direct reconstruction of wireframe models from orthogonal, axonometric projections of normalons and quasi-normalons. It is fast and accurate, Line Drawings with hidden lines can be reconstructed, and two-dimensional face calculations are not required. On the contrary, it gives poor results for non-normalons, and is very sensitive to oblique projections. Nevertheless, in many of such cases, it can still be used as a tentative model for optimisation approaches.

Axonometric Inflation does not work at all for inaccurate drawings. Hence, a pre-processing is necessary for tiding the drawings.

Finally, the automatic detection of main directions is accomplished.

Acknowledgements

References

1. Ullman D.G; Wood S and Craig D. 1990. The Importance of Drawing in the Mechanical Design Process. *Computers and Graphics*. Vol 14, No 2, pp263-274.

2. Cugini U. 1991. The problem of user interface in geometric modelling, Computers in Industry 17, 335-339.

3. Jenkins D.L. and Martin R.R. 1993. The importance of free-hand sketching in conceptual design: Automatic sketch input. *Design Theory and Methodology DTM93. T.K. Hight and L.A. Stauffer, Eds. DE-53, ASME*, pp 115-128.

4. Dori D. 1995. From engineering drawings to 3D CAD models: are we ready now? *Computer Aided Design,* vol. 27 No. 4, pp. 243-254.

5. Company, P. 1997. Integrating Creative Steps in CAD Process. *Proceedings, of the International Seminar on Principles and Methods of Engineering Design*. Napoli. Vol. 1, pp. 295-322.

6. Roberts L.G. 1963. *Machine Perception of Three-Dimensional Solids*. PhD Thesis. Massachusetts Institute of Technology.

7. Sugihara K.1986. *Machine interpretation of Line Drawings*. The MIT Press.

8. Nagendra I.V. and Gujar U.G. 1988. 3-D Objects From 2-D Orthographic Views – A Survey. *Computers & Graphics*. Vol. 12, No. 1, pp. 111-114.

9. Wang W. and Grinstein G. A. 1993. Survey of 3D Solid Reconstruction from 2D Projection Line Drawings. *Computer Graphics Forum*. Vol. 12, No 2, pp. 137-158.

10. Parodi P. 1996. "The complexity of understanding line drawing of Origami scenes" *International Journal of Computer Vision*. Vol. 18, No.2, pp.139-170.

11. Dori D. 1992. "Dimensioning Analysis. Toward Automatic Understanding of Engineering Drawings". *Communications of the ACM*, vol. 35 No. 10, pp. 92-103.

12. Marill T. 1991. "Emulating the Human Interpretation of Line-Drawings as Three-Dimensional Objects". *International Journal of Computer Vision*. Vol. 6, No. 2, pp. 147-161.

13. Lipson H. and Shpitalni M. 1996. Optimization-Based Reconstruction of a 3D Object from a Single Freehand Line Drawing. *Computer Aided Design*. Vol. 28, No. 8, pp. 651-663.

14. Leclerc Y. and Fischler M. 1992. An Optimization-Based Approach to the Interpretation of Single Line Drawings as 3D Wire Frames. *International Journal of Computer Vision*. Vol. 9, No. 2, pp. 113-136.

15. Turner A, Chapmann D. and Penn A. 2000. Sketching space. *Computer & Graphics* No 24, pp 869-879.

16. Lamb, D. and Bandopadhay, A. 1990. Interpreting a 3D object from a rough 2D line drawing *Proceedings of Visualization'90*, pp.59-66.

17. Shpitalni M. and Lipson H. 1996. Identification of Faces in a 2D Line Drawing Projection of a Wireframe Object. *IEEE Trans. Model Analysis & Machine Intell*. Vol. 18, No. 10, pp. 1000-1012.

18. Varley P.A.C. and Martin R.R. 2000. A System for Constructing Boundary Representation Solid Models from a Two-Dimensional Sketch - Frontal Geometry and Sketch Categorisation. *1st Korea-UK Joint Workshop on Geometric Modeling and Computer Graphics*.

19. Hohenberg F. 1956. *Konstruktive Geometrie für Techniker*. Wien, Springer.

20. Perkins, D.N. 1971 *Cubic Corners.* Quarterly Progress Report 89, 207-214, MIT Research Laboratory of Electronics, 1968. (See Perkins, D. *Cubic Corners, Oblique Views of Pictures, the Perception of Line Drawings of Simple Space Forms. Geometry and the Perception of Pictures: Three Studies*. Technical Report No. 5 (URL: http://pzweb.harvard.edu).)

21. Attneave F. and Frost R. 1969. The determination of perceived tridimensional orientation by minimum criteria. *Psychonomic Journals, Perception & Psychophysics* Vol. 6, pp.391-396.

22. Perkins D.N. 1976. How good a bet is good form? *Perception*, volume 5, pp 393-406.

23. Conesa J., Company P. and Gomis J.M. 1999. Initial Modeling Strategies for Geometrical Reconstruction Optimization-Based Approaches. *11th ADM International Conference on Design Tools and Methods in Industrial Engineering. Conference Proceedings. Volume A,* pp. 161-171.